SPANDIDOS PUBLICATIONS

ONCOLOGY LETTERS 29: 6, 2025

Anticancer effect of the oncolytic Newcastle disease virus harboring the PTEN gene on glioblastoma

SEONHEE KIM[1*], BO-KYOUNG JUNG[1*], JINJU KIM[1], JOO HEE JEON[1], MINSOO KIM[2], SUNG HOON JANG[3], CUK-SEONG KIM[2] and HYUN JANG[1]

[1]Research and Development Division, Libentech Co., Ltd., Daejeon 34013, Republic of Korea; [2]Department of Physiology and Medical Science, Chungnam National University College of Medicine, Daejeon 35015, Republic of Korea; [3]Graduate School of Medical Science, College of Medicine, Yonsei University, Seoul 03722, Republic of Korea

Received April 9, 2024; Accepted September 25, 2024

DOI: 10.3892/ol.2024.14752

Abstract. Glioblastoma (GBM) is one of the most lethal types of human brain cancer and is characterized by rapid growth, an aggressive nature and a poor prognosis. GBM is highly heterogeneous, and often involves several genetic mutations and abnormalities. Genetic disorders or low expression of phosphatase and tensin homolog (PTEN) are associated with GBM occurrence, progression and poor prognosis of patients with GBM. However, effective delivery of PTEN for expression in GBM cells within the brain remains challenging. The aim of the present study was to develop a therapeutic strategy to restore PTEN expression in GBM cells by utilizing a recombinant Newcastle disease virus (rNDV) vector expressing the human PTEN gene (rNDV-PTEN). Methods included infection of U87-MG cells with rNDV-PTEN, followed by assessments of PTEN expression, and cell proliferation, migration and apoptosis. Additionally, an orthotopic GBM mouse model was used to evaluate the *in vivo* efficacy of rNDV-PTEN. Infection with recombinant rNDV-PTEN treatment increased PTEN protein expression in the cytoplasm of the U87-MG cells, reduced cell proliferation and migration, and induced apoptosis by inhibiting the AKT/mTOR signaling pathway. In the orthotopic GBM mouse model, rNDV-PTEN significantly reduced tumor size and improved survival rates. Magnetic resonance imaging and *in vivo* imaging analyses confirmed the targeted delivery and efficacy of rNDV-PTEN. These findings highlight the usefulness of rNDV-PTEN as a promising therapeutic agent for GBM, representing a potential advancement in treatment, especially for patients with PTEN deficiency.

Correspondence to: Dr Hyun Jang, Research and Development Division, Libentech Co., Ltd., C-722 Daedeok BIZ Center, Techno 4-ro 17, Yuseong, Daejeon 34013, Republic of Korea
E-mail: vacchyun@naver.com

[*]Contributed equally

Key words: glioblastoma, phosphatase and tensin homolog, Newcastle disease virus, orthotopic mouse model, apoptosis

Introduction

Glioblastoma (GBM) is one of the most aggressive types of malignant primary brain tumors, accounting for ~48% of all primary malignant central nervous system tumors and ~57% of all gliomas (1). Despite the extensive use of therapeutic approaches, including surgery, radiation therapy and chemotherapy, the long-term prognosis of GBM, referring to overall survival outcomes and quality of life, remains poor, with a median survival time of ~15 months from diagnosis, primarily due to tumor recurrence and resistance to therapy (2).

One of the major challenges in treating GBM is the blood-brain barrier (BBB), a highly selective semipermeable border consisting of endothelial cells that prevent solutes in the circulating blood from non-selectively crossing into the extracellular fluid of the brain. The BBB is composed of brain microvascular endothelial cells (BMECs), astrocytes and pericytes, which together form a physical and biochemical barrier that restricts the entry of most therapeutic agents into the brain (3). Whilst the BBB allows the passage of certain small molecules through passive diffusion and the selective transport of essential nutrients and ions, it also effectively blocks larger molecules, including many chemotherapeutic drugs (4). This characteristic of the BBB poses a significant challenge for the treatment of GBM, necessitating the development of novel strategies for safe and effective drug delivery across the BBB.

Phosphatase and tensin homolog (PTEN) is a critical tumor suppressor gene that encodes a phosphatase enzyme involved in the dephosphorylation of phosphatidylinositol-3,4,5-trisphosphate, thereby negatively regulating the phosphatidylinositol 3-kinase (PI3K)/AKT/mTOR signaling pathway (5). Activation of this pathway in cancer cells promotes cell proliferation, survival, migration, angiogenesis and metastasis, whilst inhibiting apoptosis (6). Mutations that affected PTEN protein destabilization were reported to result in stronger AKT activation than mutations that affected phosphatase activity. Another patient study with PTEN gene alteration of GBM reported that the phosphatase activity of PTEN was not associated with AKT deactivation; wild-type PTEN protein expression in the

cytoplasm has been shown to be associated with decreased AKT phosphorylation, which in turn reduces AKT activity and downstream signaling, leading to suppressed cellular proliferation and survival (7). PTEN mutations or deletions are commonly observed in several cancers, including prostate cancer, endometrial cancer and GBM (8). A total of ~40% of patients with GBM exhibit PTEN deficiencies, which are associated with a poor prognosis (9). This poor prognosis includes shorter overall survival times and lower response rates to conventional therapies. PTEN acts as a tumor suppressor by negatively regulating the AKT/mTOR signaling pathway, and its loss leads to uncontrolled cell proliferation and survival. This makes PTEN a critical target for therapeutic strategies aimed at treating GBM (10). Several studies have reported that PTEN restoration in GBM cells can decrease cell proliferation and increase apoptosis, suggesting a potential therapeutic strategy (11-13). However, effective delivery systems for PTEN gene therapy in the brain have not been fully developed. Traditional delivery methods face significant obstacles owing to the BBB, which limits the entry of therapeutic agents into the brain. Innovative approaches to deliver therapeutic genes such as PTEN to GBM cells are urgently required.

Newcastle disease virus (NDV) is an intrinsic oncolytic virus that selectively replicates in tumor cells without affecting normal cells (14). NDV induces cancer cell death through mechanisms such as apoptosis, autophagy and necroptosis and can stimulate the host immune response against cancer by releasing cytokines and chemokines that attract immune cells to the tumor site (14). This characteristic makes NDV a promising candidate for oncolytic virotherapy, particularly for tumors such as GBM, which are difficult to treat with conventional therapies. NDV has shown promise in clinical trials for the treatment of several cancers, including GBM (15,16). In a previous study, intravenous administration of NDV in patients with recurrent GBM resulted in a marked reduction in tumor size and mild adverse reactions comparable with the symptoms of influenza (17). However, the precise mechanism by which NDV crosses the BBB remains unclear. NDV may exploit pathways similar to those used by other viruses, such as severe acute respiratory syndrome coronavirus 2 (SARS-CoV-2), which infect brain vascular endothelial cells and cross the BBB (18). Astrocytes, which are in direct contact with the outer surface of brain blood vessel endothelial cells, may serve as a conduit for viral entry into the brain (19).

Our previous study constructed a recombinant NDV expressing human PTEN (rNDV-PTEN) and demonstrated its ability to inhibit GBM cell growth *in vitro* and in a xenograft animal model (20). The recombinant virus combined the tumor-selective replication properties of NDV with the tumor-suppressive functions of PTEN, thereby providing an increasing GBM cell death of GBM cells. Therefore, the present study aimed to build on these findings by evaluating the therapeutic potential of rNDV-PTEN in an orthotopic mouse model of GBM, focusing on its ability to cross the BBB and deliver PTEN to GBM cells. Through these comprehensive analyses, the present study aimed to provide a detailed understanding of the potential use of rNDV-PTEN as a therapeutic agent for GBM. Furthermore, the present study aimed to develop an effective treatment strategy that overcomes the limitations imposed by the BBB and improves the prognosis of patients with this disease.

Materials and methods

Cell culture and cell growth. Human GBM cells, U87-MG (cat no. HTB-14; GBM of unknown origin), U87-MG-luc2 (cat. no. HTB-14-LUC2; GBM of unknown origin), T98G (cat. no. CRL-1690) and CCF-STTG1 (cat. no. CRL-1718), were purchased from American Type Culture Collection (ATCC). Proneural X01 (21) and Mensenchymal 83 (22) cells were donated by Professor Park Jong Bae's team at the Korea National Cancer Center (23). The passage number at which these cells were supplied was passage 11 and the cells were experimentally used starting from passage 14.

U87-MG, U87-MG-luc2, T98G and CCF-STTG1 cells were cultured in high-glucose Dulbecco's modified Eagle's medium (DMEM; Gibco; Thermo Fisher Scientific, Inc.) containing 10% heat-inactivated fetal bovine serum (FBS; Sigma-Aldrich; Merck KGaA) and 1% penicillin-streptomycin (Gibco; Thermo Fisher Scientific, Inc.) and maintained at 37˚C in humidified air with 5% CO_2.

Proneural X01 and were cultured in DMEM/F12 (Gibco; Thermo Fisher Scientific, Inc.) supplemented with 10 ng/ml epidermal growth factor (cat. no. 236-EG; R&D Systems, Inc.), basic fibroblast growth factor (cat. no. 4114-TC; 5 ng/ml for Proneural X01 and 10 ng/ml for Mesenchymal 83; R&D Systems, Inc.). B27 (Invitrogen™; Thermo Fisher Scientific, Inc.) and 1% penicillin-streptomycin (Gibco; Thermo Fisher Scientific, Inc.), and maintained at 37˚C in humidified air with 5% CO_2.

rNDV-PTEN virus was previously constructed (20). The virus was propagated by infection of vero cells (CCL-81; ATCC) at a multiplicity of infection (MOI) of 0.5 for 2 days prior (20). The virus titer was tested by the 50% tissue culture infective dose ($TCID_{50}$/ml) method of Spearman and Kärber (24,25).

Sample preparation. U87-MG and CCF-STTG1 cells ($1x10^7$ cells) seeded in a 175T flask were cultured overnight at 37˚C in humidified air with 5% CO_2. The cells were infected with rNDV or rNDV-PTEN viruses at an MOI of 1.0 for 1 h, washed two times with PBS and then incubated for 12-36 h at 37˚C in humidified air with 5% CO_2, with DMEM containing 10% FBS and 1% penicillin-streptomycin. The supernatant was removed and cells were collected at 12, 24 and 36 h after virus infection and the cells were subjected to three freezing/thawing cycles at -80˚C and 4˚C. The cell lysates were used for quantitative (q)PCR and immunoblot analysis.

Animal studies. Female BALB/c nu-/nu- mice (n=40; 5 weeks old), weighing ~18-20 g, were purchased from Orient Bio, Inc. The mice were housed under standard conditions with a 12-h light/dark cycle, a temperature of 22±2˚C and a humidity of 55±10%, with food and water provided *ad libitum*. For anesthesia, each mouse was weighed to calculate the appropriate dose of 2,2,2-tribromoethanol (Avertin®) via intraperitoneal administration at 250 mg/kg.

U87-MG cells were cultured in DMEM (Gibco; Thermo Fisher Scientific, Inc.) containing 10% heat-inactivated FBS (Sigma-Aldrich; Merck KGaA) and 1% penicillin-streptomycin (Gibco; Thermo Fisher Scientific, Inc.), and maintained at 37˚C in humidified air with 5% CO_2. Before injection, U87-MG cells

were trypsinized, counted and resuspended in growing media. The cell suspension was kept on ice until the time of injection. Each mouse was injected with $5x10^4$ U87-MG cells in 5 μl ($1x10^4$ cells/μl) as follows: A midline incision of ~1.2 cm was made. A small hole was drilled in the skull at the point 0.2 mm back and 2.2 mm to the left of the bregma. Cell suspensions were injected with a Hamilton syringe at a rate of 1 μl/min, and the syringe was left in place for 5 min. The mice were screened using an *in vivo* imaging system (IVIS) every 7 days. After 40 days, the mice were randomly divided them into three groups (n=4 per group): rNDV (100 μl 10^7 $TCID_{50}$/dose, intravenous), rNDV-PTEN (100 μl 10^7 $TCID_{50}$/dose, intravenous) and PBS as a negative control.

Immunoblotting. For immunoblotting, proteins were extracted using RIPA buffer (Thermo Fisher Scientific, Inc.) containing 50 mM Tris-HCl (pH 7.4), 150 mM NaCl, 1% NP-40, 0.5% sodium deoxycholate and 0.1% SDS. Protein concentration was determined using the bicinchoninic acid method. Equal amounts of protein (30 μg) were loaded per lane on a 15% SDS-PAGE gel. Proteins were then transferred to a polyvinylidene difluoride membrane. The membrane was blocked with 5% non-fat dry milk in TBS-T (0.1% Tween-20) for 1 h at room temperature. The membranes were incubated overnight at 4°C with the following primary antibodies: Anti-GAPDH (1:3,000; cat. no. sc-32233; Santa Cruz Biotechnology, Inc.); anti-LC3 (1:1,000; cat. no. NB100-2220; Novus Biologicals, LLC); anti-matrix metallopeptidase 9 (MMP9; 1:1,000; cat. no. MA5-15886; Thermo Fisher Scientific, Inc.); anti-proliferating cell nuclear antigen (PCNA; 1:500; cat. no. PC 10; Sigma-Aldrich; Merck KGaA); anti-P-mTOR (Ser2448; 1:1,000; cat. no. 2971S; Cell Signaling Technology, Inc.); anti-mTOR (1:1,000; cat. no. 2972S; Cell Signaling Technology, Inc.); anti-P-Akt (Ser473; 1:1,000; cat. no. 9271S; Cell Signaling Technology, Inc.); anti-Akt (1:1,000; cat. no. 9272S; Cell Signaling Technology, Inc.); anti-cleaved Caspase (Cas)9 (1:1,000; cat. no. 9509S; Cell Signaling Technology, Inc.); anti-cleaved Cas3 (1:1,000; cat. no. 9664S; Cell Signaling Technology, Inc.); anti-cleaved Cas8 (1:1,000; cat. no. 9496S; Cell Signaling Technology, Inc.); anti-B-cell lymphoma 2 (Bcl-2) associated X protein (Bax; 1:1,000; cat. no. 2772S; Cell Signaling Technology, Inc.); anti-p62 (1:1,000; cat. no. 5114S; Cell Signaling Technology, Inc.); anti-Occludin (1:1,000; cat. no. 5506S; Cell Signaling Technology, Inc.); anti-zonula occludens protein 1 (ZO-1; 1:1,000; cat. no. 5406S; Cell Signaling Technology, Inc.); anti-Clauddin-5 (E8F3D; 1:1,000; cat. no. 49564; Cell Signaling Technology, Inc.); and anti-PTEN (1:1,000; cat. no. 9552S; Cell Signaling Technology, Inc.). After washing with TBS-T (0.1% Tween 20), the membranes were incubated with horseradish peroxidase-conjugated secondary antibodies (Anti-Rabbit, cat. no. 7074S; and Anti-Mouse, cat. no. 7076S; 1:5,000; Cell Signaling Technology, Inc.) for 1 h at room temperature. Proteins were visualized using the Pierce™ ECL Western Blotting Substrate (cat. no. 32106; Thermo Fisher Scientific, Inc.). Values were normalized to GAPDH as loading controls. Protein levels were semi-quantified using densitometric analysis using Image J software (version 1.49; National Institutes of Health).

RNA extraction and reverse transcription-qPCR. Total RNA was isolated using TRIzol™ Reagent (Invitrogen; Thermo Fisher Scientific, Inc.) based on the acid guanidinium thiocyanate-phenol-chloroform method. Total RNA concentration was determined using a spectrophotometer (Nano Drop™ 2000/2000c Spectrophotometer; Thermo Fisher Scientific, Inc.). Complementary DNA was prepared from total RNA (1 μg) using the RevertAid First Strand cDNA Synthesis Kit (cat. no. K1622; Thermo Fisher Scientific, Inc.). The thermocycling conditions for cDNA synthesis were as follows: 65°C for 5 min, 55°C for 50 min and 85°C for 5 min. qPCR was then performed using the StepOnePlus™ Real-Time PCR system (Bio-Rad Laboratories, Inc.) with the SYBR® Premix Ex Taq™ kit (cat. no. RR820A; Takara Bio, Inc.). The thermocycling conditions for qPCR were as follows: Initial denaturation, 95°C for 5 sec; followed by 35 cycles of denaturation at 94°C for 15 sec, annealing at 55°C for 25 sec and extension at 70°C for 30 sec. The primers used for human PTEN were as follows: Sense, 5'-CAAGATGATGTTTGAAACTAT-3' and antisense, 5'-CCTTTAGCTGGCAGACCACAA-3'. The primers used for mouse Occludin were as follows: Sense, 5'-ACTGGG TCAGGGAATATCCA-3' and antisense, 5'-TCAGCAGCA GCCATGTACTC-3'. The primers used for mouse ZO-1 were as follows: Sense, 5'-AGGCTACCTTTGTATTCTC-3' and antisense, 5'-TAGGGCACAGTATTGTATC-3'. The primers used for mouse Claudin-5 were as follows: Sense, 5'-CTT CCTGGACCACAACATCGTG-3' and antisense, 5'-CACGTC GGATCATAGAACTCG-3'. The primers for human 18s, used as the internal control, were as follows: Sense, 5'-GTAACC CGTTGAACCCCATT-3' and antisense, 5'-CCATCCAATC GGTAGTAGCG-3'. The primers for mouse 18s, used as the internal control, were as follows: Sense, 5'-GAGCGACCA AAGGAACCATA-3' and antisense, 5'-CGCTTCCTTACC TGGTTGAT-3'. Dissociation curves were monitored to assess the aberrant formation of primer-dimers. The fold change in the interest gene expression was calculated using the $2^{-\Delta\Delta Cq}$ method (26).

Histological analysis. Brain tissues from the orthotopic GBM model were fixed with 4% (w/v) paraformaldehyde at room temperature for 24 h. The fixed tissues were then embedded in paraffin and sectioned into 5 μm-thick slices. The sections were deparaffinized using xylene, followed by rehydration through a graded series of alcohols (100, 80 and 70%), and finally rinsed in PBS. Next, hematoxylin and eosin staining was performed by incubating the sections in hematoxylin for 5 min at room temperature, followed by eosin for 2 min at room temperature. For immunohistochemistry staining, tumor tissue sections were fixed with 10% neutral buffered formalin at room temperature for 24 h. After fixation, the sections were embedded in paraffin using standard procedures. Tumor sections of a 5-μm thickness were cut and mounted on slides. For antigen retrieval, sections were treated with sodium citrate buffer (pH 6.0; cat. no. C999; MilliporeSigma) and heated in a microwave for 3 min at 95°C. After retrieval, the sections were rehydrated through a descending alcohol series (100, 80 and 70% ethanol) and washed in PBS. The sections were blocked with 1% bovine serum albumin (cat. no. 4378; MilliporeSigma) in PBS for 1 h at room temperature, and then stained with

the following primary antibodies: Anti-MMP9 (1:100; cat. no. MA5-15886; Thermo Fisher Scientific, Inc.), anti-PTEN (1:200; cat. no. 9559S; Cell Signaling Technology, Inc.) anti-NDV hemagglutinin-neuraminidase protein (1:200; HN; cat. no. sc-53562; Santa Cruz Biotechnology, Inc.) and anti-Ki-67 (1:100; cat. no. MA5-14520; Thermo Fisher Scientific, Inc.) overnight at 4˚C. HRP-conjugated anti-rabbit or anti-mouse IgG secondary antibodies (cat. nos. AP160P and 12-348; MilliporeSigma) were then applied for 60 min at room temperature. Color was developed for 30 sec by incubation with DAB. Sections were counterstained with hematoxylin at room temperature for 3 min and observed under a light microscope (Motic Instruments) at x100 magnification.

Cell Counting Kit-8 (CCK-8) cell proliferation assay. CCF-STTG1, U87-MG, T98G, Mesenchymal 83 and Proneural X01 cells were seeded at $1x10^4$ cells/well in 96-well plates (cat. no. 34096; SPL Life Sciences). On the next day, the cells were treated with rNDV-PTEN or rNDV (0.3, 1 or 3 MOI) for 24 h. Cell proliferation was measured using a CCK-8 kit (cat. no. CK04-1000; Dojindo Laboratories, Inc.) according to the manufacturer's instructions. Briefly, cells were washed with PBS and suspended in growth medium including CCK-8 reagent added at 1/100 the media volume. Cells were then incubated at 37˚C for 1 h in the dark. Cell proliferation was measured at a wavelength of 450 nm.

TUNEL assay. A TUNEL assay was used to detect DNA fragmentation, such as apoptosis. U87-MG cells were seeded at $1x10^5$ cells/well in a 6-well plate (cat. no. 30006; SPL Life Sciences). Cells were treated with rNDV-PTEN or rNDV (1 MOI) for 24 h. After 24 h of incubation at 37˚C with 5% CO_2, the cells were washed twice with PBS, detached from the plate using trypsin and collected in a 15 ml tube. These cells were fixed in 100% ethanol overnight at 4˚C. A TUNEL assay was performed according to the manufacturer's instructions (TUNEL Assay Kit-FITC; cat. no. ab66108; Abcam). Following fixation, the cells were permeabilized with 0.1% Triton X-100 in PBS for 2 min on ice. The cells were then incubated with FITC-labeled dUTP in the presence of terminal deoxynucleotidyl transferase at 37˚C for 1 h. Stained cells were analyzed using flow cytometry and fluorescence for FITC using a NovoCyte Quanteon flow cytometer (Agilent Technologies, Inc.) and fluorescence microscope (Zeiss Axio Imager M1; Zeiss GmbH) as per the manufacturer's instructions (Agilent Technologies, Inc.). Data acquisition was performed using a flow cytometer (FACS; NovoCyte Quanteon flow cytometer; Agilent Technologies, Inc.), measuring PE-A fluorescence intensity, and ~1,000 cells per sample were analyzed to determine the extent of apoptosis. Flow cytometry data were analyzed using NovoExpress software (version 1.6.2; https://www.agilent.com/ko-kr/product/research-flow-cytometry/flow-cytometry-software/novocyte-novoexpress-software-1320805). After completing the FACS experiment, 100 μl of the stained cells were transferred onto a cover slide. The cells were then assessed using fluorescence microscopy (ZEISS LSM 980; Zeiss GmbH) to evaluate and visualize the expression and localization of the TUNEL (FITC).

Transwell assay. A Transwell assay was used to assess cell migration. U87-MG cells were seeded at $1x10^5$ cells/well, with uninfected cells (CON) or rNDV (1 MOI) or rNDV-PTEN (1 MOI), into 6-well tissue culture plates for 24 h, followed by transfer of $5x10^5$/ml cells in the upper Transwell chamber (24-well plate; Corning, Inc.) and cultured with FBS-free medium at 37˚C, with 5% CO_2. Complete growth medium with 10% FBS (Merck KGaA) was added to the lower chamber and incubated for another 24 h at 37˚C, with 5% CO_2. Cells on the upper side (non-migrating cells) were then removed and migrated cells on the lower face were washed with PBS, fixed with 4% paraformaldehyde at room temperature for 15 min, and stained with DAPI at room temperature for 10 min. The cells were counted in 5 random high-power fields (x200 magnification) under a microscope (ZEISS LSM 980; Zeiss GmbH) and averaged.

IVIS. Mice were anesthetized with 2.5% isoflurane for induction and maintained with 1.5% isoflurane until the completion of IVIS imaging. Luciferase imaging was performed using an *in vivo* optical imaging system (IVIS Lumina XR; PerkinElmer, Inc.) 15 min after intraperitoneal injection of 100 μl Luciferin (30 mg/ml). The images were captured and then the signal was displayed as Radiant Efficiency (Photons/sec/cm^2/steradium (sr) or μW/cm^2). Images of the region-of interest were analyzed using the Living imaging 4.4 software (PerkinElmer, Inc.).

Magnetic resonance imaging (MRI). Mice were transferred to the MRI unit using individual portable cages within 30 min of anesthesia with 2.5% isoflurane. Using a 32-channel phased array sensitivity encoding head coil, MRI imaging was performed on the anesthetized mice with a 7.0 Tesla Philips MR scanner (Ingenia; Philips Healthcare). Each mouse was scanned in the upright position with a coil over its head. Mice were mainlined under anesthesia with 1% isoflurane. The following parameters were used for acquisition of the multi-shot echo-planar imaging fast spin echo, with image reconstruction using image-space sampling functions with b-values of 0 and 1,000 s/mm^2, and 3 orthogonal directions of diffusion gradients: Echo time, 45 msec; repetition time, 5,000 msec; slice thickness, 8 mm; interslice gap, 1 mm; number of averaging, =2; bandwidth, 936 Hz/pixel; echo train length, 35; field of view, 25.0x25.0 cm; and matrix size, 256x256 pixels.

Statistical analysis. Statistical analysis was performed using Prism 8 software (Dotmatics). Data are presented as mean ± standard deviation. Differences between two groups were evaluated using unpaired t-tests. For multiple comparisons, one-way analysis of variance was performed followed by Tukey's multiple comparison test. $P<0.05$ were considered to indicate a statistically significant difference. Data are representative of at least three independent experiments.

Results

Restoration of PTEN via NDV attenuates the proliferation of U87-MG cells. A significant decrease in PTEN expression was demonstrated in the U87-MG GBM cell line in comparison with normal brain cells (astrocytes: CCF-STTG1). PTEN expression in other GBM cell lines (T98G, Proneural X01

and Mesenchymal 83 cells) did not demonstrate a significant decrease compared with astrocytes (Fig. 1A and B). Therefore, U87-MG cells were chosen as the primary focus for assessing the anticancer effects of PTEN restoration.

The present study constructed rNDV-PTEN (20) to induce PTEN mRNA and protein expression in the cytoplasm of U87-MG and CCF-STTG1 cells. In normal cells, such as astrocytes, the Type I interferon (IFN) pathway, particularly IFN-α, is active and effectively inhibits viral replication by inducing an antiviral state, preventing the proliferation of NDV. By contrast, cancer cells like those in GBM often have a compromised IFN-α signaling pathway due to the deletion of the cyclin-dependent kinase inhibitor 2A and Type I IFN gene cluster (15). This impairment allows NDV to replicate efficiently within cancer cells, leading to selective oncolysis. Therefore, IFN-α serves a critical role in maintaining antiviral defenses in normal cells, whereas its dysfunction in cancer cells enables the oncolytic activity of the virus (27). The results of the present study demonstrate that in CCF-STTG1 cells, the virus did not exhibit oncolytic activity, resulting in no significant change in cell proliferation compared with GBM cell lines. However, in GBM cell lines, there was a greater reduction in cell proliferation with increased virus exposure time or when treated with rNDV-PTEN, which contains the inserted PTEN gene. Statistical analysis revealed a significant reduction in cell proliferation in GBM cell lines compared with that in untreated cells (Fig. 1C). The reason for using the PTEN gene is that 40% of patients with GBM have PTEN gene mutations, as well as the U87-MG cell line we used. These mutations lead to the dysfunction of the PTEN protein, which is associated with a worse prognosis in GBM (28-30). Therefore, the present study aimed to enhance the therapeutic effect on GBM by delivering and expressing the PTEN gene through rNDV-PTEN. Treatment with rNDV-PTEN significantly suppressed the proliferation of U87-MG cells in comparison with its effects in the CCF-STTG1 and other GBM cell lines (Fig. 1C). Furthermore, the present study assessed the NDV-HN protein in astrocyte cells (CCF-STTG1) and GBM cell lines in samples that were either untreated (0 h, no treatment) or treated (36 h, rNDV-PTEN virus). The results revealed that in astrocytes (CCF-STTG1), the expression of the NDV-HN protein was significantly lower compared with that in the other GBM cell lines (Fig. S1). Taken together, U87-MG cells were selected for further assessment of the anticancer effects of rNDV-PTEN.

A Transwell assay to evaluate U87-MG cell migration revealed that most of the rNDV-PTEN-treated cells did not migrate to the lower chamber containing the complete medium. Further analysis, including DAPI staining of migrated cells, followed by microscopic counting, demonstrated significantly decreased migration (Fig. 1D). To assess the mechanism through which PTEN restoration induces apoptosis in U87-MG cells, a TUNEL assay was performed (Fig. 1E). TUNEL-positive cells were observed in both rNDV and rNDV-PTEN, with rNDV-PTEN treatment associated with ~2.5x more positive cells compared with rNDV. The TUNEL assay (FITC) was performed using FACS and cell staining was evaluated with a fluorescence microscope on a cover slide (Fig. S2). These findings indicate that rNDV-PTEN treatment inhibited the migration of U87-MG cells and induced DNA fragmentation, leading to apoptosis.

Restoration of PTEN via NDV regulates AKT/mTOR pathway and increases apoptosis of U87-MG GBM cells. The deactivation (dephosphorylation) of AKT/mTOR and apoptosis-associated signaling pathways in U87-MG cells were also analyzed using immunoblot analysis. Specifically, these cells were infected with rNDV or rNDV-PTEN at a MOI of 1 and collected for analysis at 12, 24 and 36 h post-infection (hpi). The results revealed that in comparison with the PTEN bands in rNDV-infected cells, those in rNDV-PTEN-infected cells gradually increased between 12 and 36 hpi and peaked at 36 hpi, indicating active virus replication, with a significant increase in PTEN expression over time (Fig. 2A). Additionally, the levels of PCNA were assessed, a well-conserved protein in eukaryotes and a proliferation marker expressed in cells undergoing division (31). The level of MMP9 was also evaluated, which serves an essential role in local proteolysis of the extracellular matrix and in leukocyte migration (32,33). The results demonstrated decreased PCNA and MMP9 expression levels in rNDV-PTEN-infected U87-MG cells compared with those in uninfected cells (Fig. 2A). Additionally, the activation of AKT/mTOR, as the endpoint of the PI3K pathway, contributes to the malignant transformation of cells in several cancers (34). In the present study, AKT and mTOR phosphorylation in cells infected with rNDV or rNDV-PTEN were assessed. The results revealed that rNDV-PTEN treatment decreased the levels of phosphorylated AKT and mTOR in a dose-dependent manner (Fig. 2B). Furthermore, an increase in the levels of Bax and cleaved caspases 3, 8 and 9 were demonstrated, along with a decrease in the level of Bcl-2 in rNDV-PTEN-infected cells, compared with that in uninfected cells, indicating that this treatment induced apoptosis in GBM cells (Fig. 2C).

rNDV-PTEN treatment suppresses cancer growth in an orthotopic mouse model of GBM. To determine whether PTEN restoration significantly suppresses U87-MG cell proliferation in an *in vivo* preclinical mouse model and *in vitro*, U87-MG-Luc2 cells were orthotopically xenografted into BALB/c nude mice (Fig. 3A). A total of 40 days after tumor injection, virotherapy was initiated using intravenous injections of rNDV-PTEN, rNDV or PBS (CON). The body weight (Fig. 3B) and survival rates (Fig. 3C) of the mice were also monitored during the treatment period. To measure the *in vivo* efficacy of PTEN restoration for tumor growth suppression in GBM mouse models, the MRI findings and IVIS assessments of luciferase activity in tumor scans were compared at 1-8 weeks after tumor injection.

The results indicated weight loss was associated with tumor progression rather than survival rate in the GBM orthotopic mouse model (Fig. 3B). The treatment group that received virotherapy experienced significantly less weight loss compared with the control group mice (PBS). Furthermore, whilst all control mice died by day 60 post-tumor establishment, the rNDV and rNDV-PTEN treated mice had survival rates of 50 and 70%, respectively (Fig. 3C). MRI and IVIS assessments also demonstrated markedly lower tumor growth in rNDV-PTEN-treated mice than in rNDV- and PBS-treated mice (Fig. 3D and E). Moreover, the level of NDV-HN in the brain tumor tissues of rNDV- and rNDV-PTEN-treated mice was significantly greater than that in the brain tissue of PBS-treated mice (Fig. 4A). This

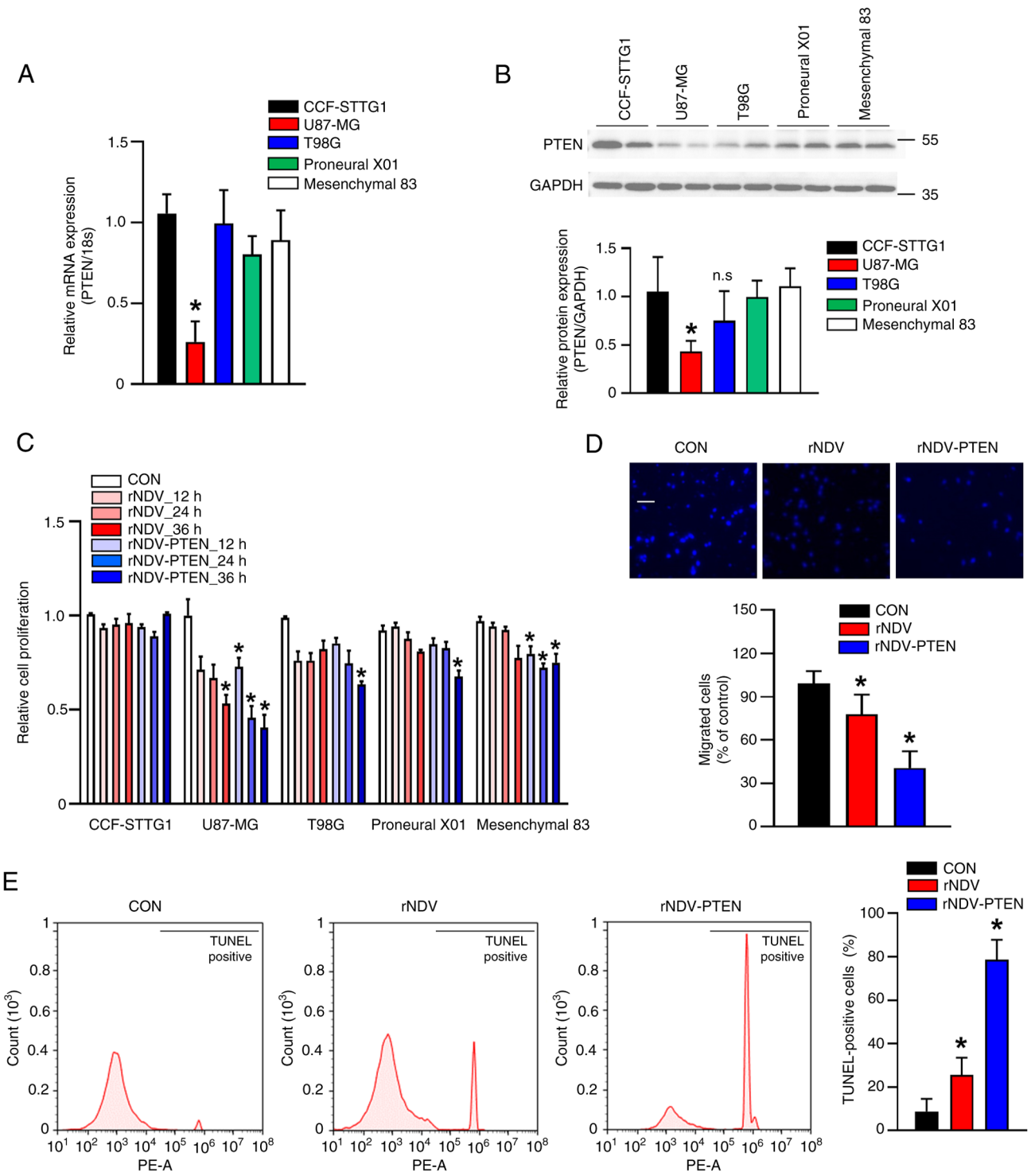

Figure 1. mRNA expression and protein expression of PTEN in normal astrocyte or GBM cell lines, and inhibition by rNDV-PTEN of cell viability and migration by inducing apoptotic cell death in U87-MG cells. PTEN (A) mRNA and (B) protein expression in normal astrocyte (CCF-STTG1) and GBM cell lines (U87-MG, T98G, Proneural X01 and Mesenchymal 83). CCF-STTG1 cells and U87-MG cells were infected rNDV or rNDV-PTEN 1 MOI for 36 h. (C) Cell viability assay performed using CCF-STTG1 cells and GBM cell lines with rNDV or rNDV-PTEN 1 MOI treatment using a Cell Counting Kit-8 Kit. (D) U87-MG cells were infected with rNDV or rNDV-PTEN and a Transwell assay was performed to assess cell migration. Cells migrated from the upper chamber to the lower chamber were stained with DAPI. Scale bar, 50 μm. (E) Apoptosis (DNA fragmentation) in U87-MG cells measured using TUNEL staining after virus infection. *P<0.05 vs. CCF-STTG1 or CON. PTEN, phosphatase and tensin homolog; GBM, glioblastoma; rNDV, recombinant Newcastle disease virus; MOI, multiplicity of infection; CON, control; n.s., not significant.

was further supported by the higher infection rate of rNDV-PTEN observed through HN staining in Fig. 4A. The mRNA and protein expression levels of tight junction proteins such as ZO-1, claudin-5 and occludin were also assessed; however, the expression levels did not significantly change in the brain tissue of mock mice models or tumor tissues in rNDV-PTEN, rNDV and PBS-treated mice (Fig. S3). This indicates that NDV crosses the BBB to reach the tumor tissue without disrupting tight junctions.

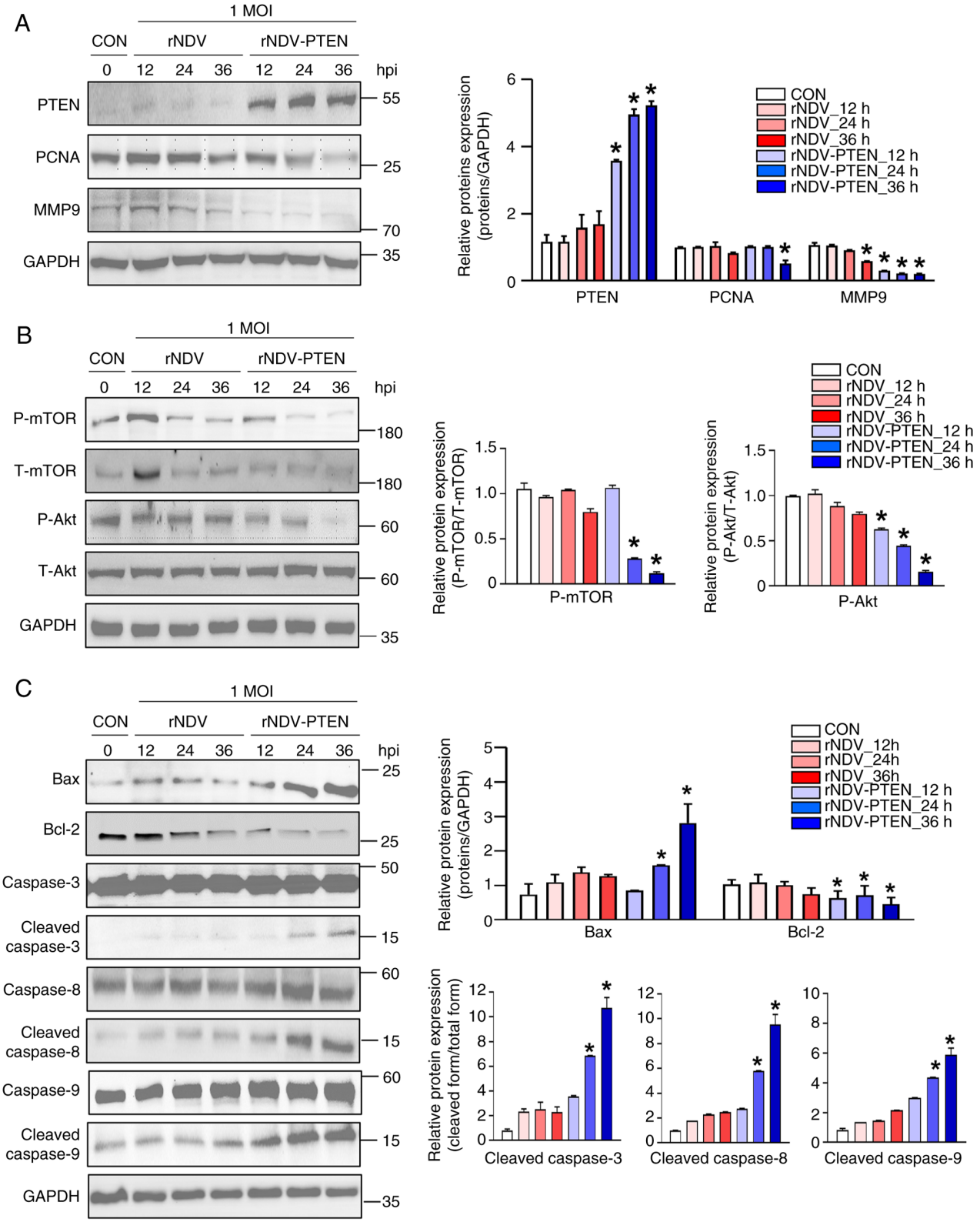

Figure 2. Effect of rNDV-PTEN infection on apoptotic cell death through imbalance of Akt/mTOR pathway. U87-MG cells were infected with rNDV or rNDV-PTEN at an MOI of 1 for 12, 24 or 36 h. (A) Cell proliferation markers PCNA and MMP9, (B) mTOR signaling-related proteins and autophagy-related proteins and (C) pre-apoptotic cell death-related proteins were assessed using immunoblotting analysis in U87-MG cells. GAPDH was used as an internal control. *P<0.05 vs. CON. rNDV, recombinant Newcastle disease virus; PTEN, phosphatase and tensin homolog; PCNA, proliferating cell nuclear antigen; MMP9, matrix metallopeptidase 9; MOI, multiplicity of infection; CON, control; Bcl-2, B-cell lymphoma 2; Bax, Bcl-2-associated X protein.

Immunohistochemical analysis was used to assess whether PTEN expression was upregulated in GBM tissues. The brains of rNDV-PTEN-treated mice exhibited significantly higher PTEN expression levels than those of PBS-treated mice (Fig. 4A). This finding indicates that the treatment with rNDV and rNDV-PTEN successfully led to the presence and activity

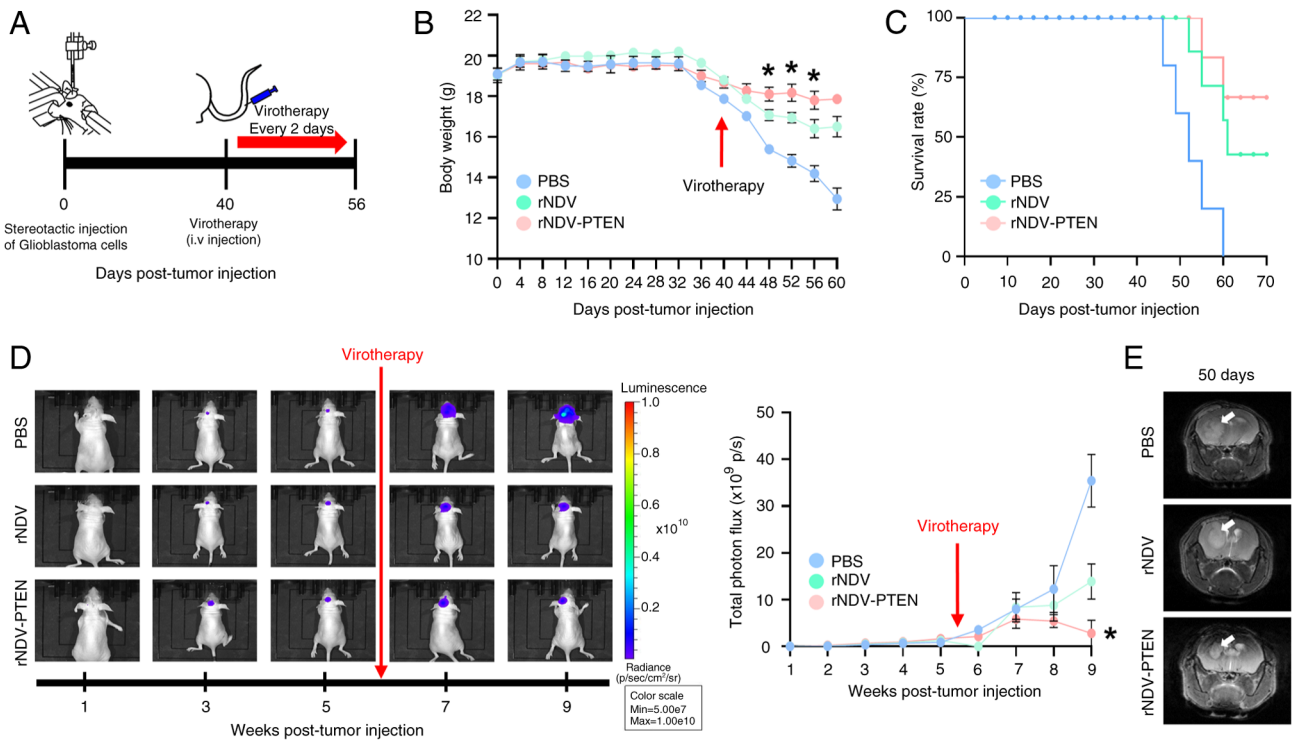

Figure 3. PTEN restoration suppresses tumorigenesis in orthotopic GBM mouse through infection of rNDV. (A) Mice were orthotopically injected with U87-MG-Luc2 cells. A total of 40 days after tumor cell injection, the mice were infected with rNDV-PTEN or rNDV via i.v. injection. (B) Body weight of *in vivo* mouse GBM models. (C) Survival rate of orthotopic GBM mouse models following rNDV-PTEN, rNDV or PBS injections (n=5). (D) Bioluminescent images of luciferase activity. Bioluminescent images were taken with IVIS Lumina XR and analyzed using Living Image Software (n=5). (E) MRI in orthotopic GBM mouse models. Representative MRI image of orthotopic GBM mouse models, taken 50 days after tumor injection (rNDV-PTEN, rNDV or PBS was injected 5 times). These data are expressed as the fold change in expression compared with PBS injected mice. *P<0.05 vs. PBS-injected mice. PTEN, phosphatase and tensin homolog; GBM, glioblastoma; rNDV, recombinant Newcastle disease virus; MRI, magnetic resonance imaging; i.v., intravenous.

of the NDV virus within the brain tumor tissues. The increased levels of NDV-HN in rNDV- and rNDV-PTEN-treated mice compared with PBS-treated mice is shown in Fig. 4A. These increases were statistically significant, indicating a meaningful difference in NDV-HN and PTEN levels between the treated and control groups, suggesting effective viral targeting and replication in the tumor environment. This indicates that the virus actively engaged with the tumor cells, potentially leading to oncolytic effects, which were absent in the PBS-treated group. The elevated presence of the viral protein in the treated mice demonstrates the potential of rNDV and rNDV-PTEN as therapeutic agents capable of reaching and affecting tumor sites within the brain. Immunoblotting performed to assess PTEN expression in cancerous and normal tissues in the brain and other tissues revealed that NDV injected into the tail vein did not affect PTEN expression in other organs compared with that in PBS-treated mice, but significantly upregulated PTEN expression in brain cancer cells (Fig. 4B and C).

Staining of brain sections with antibodies against Ki-67 and MMP9 significantly markedly lower cancer cell proliferation and migration indices (brown) in rNDV-PTEN-treated mice than in rNDV- and PBS-treated mice (Fig. 5A). Furthermore, analysis of PCNA and MMP9 protein expression levels demonstrated similar results (Fig. 5B). To elucidate the mechanism by which rNDV-PTEN treatment induces apoptosis, the regulation of the AKT/mTOR signaling pathway in GBM mouse models was evaluated. The phosphorylation levels of AKT and mTOR were significantly reduced in rNDV-PTEN-treated mice compared with those in PBS-treated or rNDV-treated mice (Fig. 5C). Changes in apoptotic protein markers were also assessed and significantly increased levels of cleaved caspases 3, 8 and 9 and Bax, and decreased levels of Bcl-2 were demonstrated in rNDV-PTEN-treated mice compared with those in PBS-treated mice. This observation indicates the activation of apoptosis in the rNDV-PTEN-treated group (Fig. 5D). Taken together, the results suggest that PTEN restoration induces apoptosis during GBM cell proliferation and migration by disrupting the AKT/mTOR signaling pathway.

Discussion

GBM remains one of the most challenging brain tumors to treat due to its aggressive nature and the protective role of the BBB, which limits the effectiveness of traditional therapies such as surgery, radiation therapy and chemotherapy. Despite these interventions, GBM often recurs, and patient prognosis remains poor, with a median survival of ~15 months from diagnosis (35). This highlights the urgent need for novel therapeutic strategies that can effectively target GBM cells and overcome the BBB.

The current delivery system for NDV offers several advantages over traditional delivery methods like those used for herpes simplex virus (HSV) and adeno-associated virus (AAV) (36). Unlike HSV and AAV, which often require direct injection into tumors for effective delivery, NDV can be administered intravenously (37,38). This

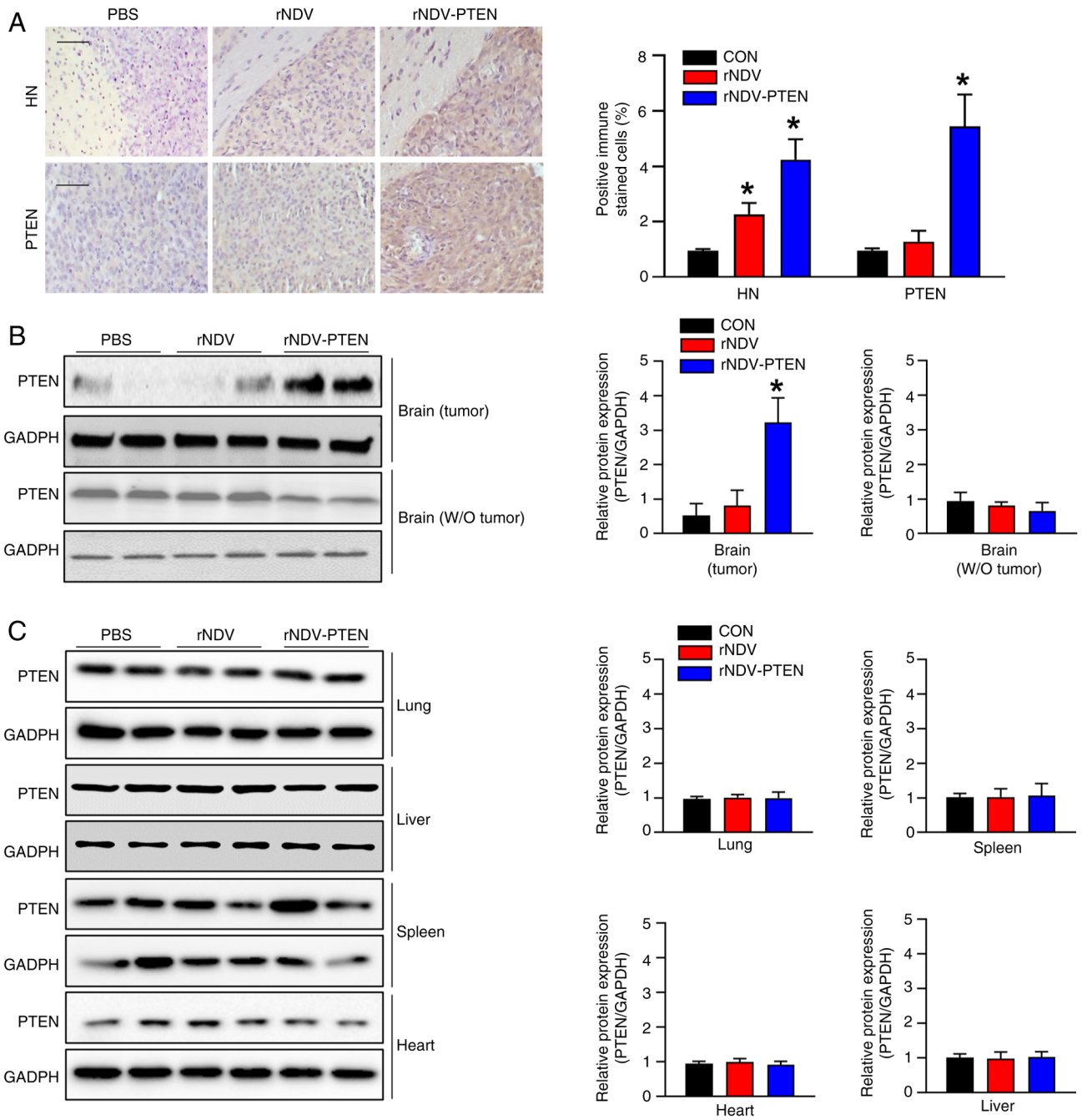

Figure 4. rNDV passes through blood-brain barrier and selectively replicates GBM without altering other tissues in the orthotopic GBM mouse model. (A) Immunohistochemical staining of HN and PTEN in the orthotopic mouse GBM tissue in brain. Scale bar, 50 μm. (B) PTEN expression was assessed using immunoblotting in GBM tissue. (C) PTEN expression was assessed using immunoblotting in major tissues. GAPDH was used as an internal control. These data are expressed as the fold change in expression compared with PBS-injected mice. *P<0.05 vs. PBS-injected mice. rNDV, recombinant Newcastle disease virus; GBM, glioblastoma; PTEN, phosphatase and tensin homolog; HN, CON, control; W/O, without.

capability allows NDV to circulate through the bloodstream and reach metastatic sites that are difficult to access with direct injections, thereby enhancing its therapeutic reach and efficacy (39). Furthermore, NDV demonstrates a high level of tumor selectivity and low immunogenicity, reducing the risk of adverse effects on normal tissues (40). Clinical trials have reported that NDV can be effectively delivered systemically, offering a more versatile and patient-friendly approach compared with localized injection strategies (41). These characteristics make NDV a superior choice for treating cancers that are not easily accessible by direct injection, highlighting its potential as an effective and innovative viral therapy (42).

The present study assessed the therapeutic potential of an rNDV-PTEN in treating GBM. The use of oncolytic viruses like NDV offers a promising approach due to their ability to selectively replicate in and kill tumor cells whilst sparing normal cells. However, several limitations should be acknowledged in the present study. Firstly, the study was conducted in a preclinical setting using *in vitro* and animal models, which may not fully replicate the complexity of human glioblastoma. Further clinical trials are necessary to validate the efficacy and

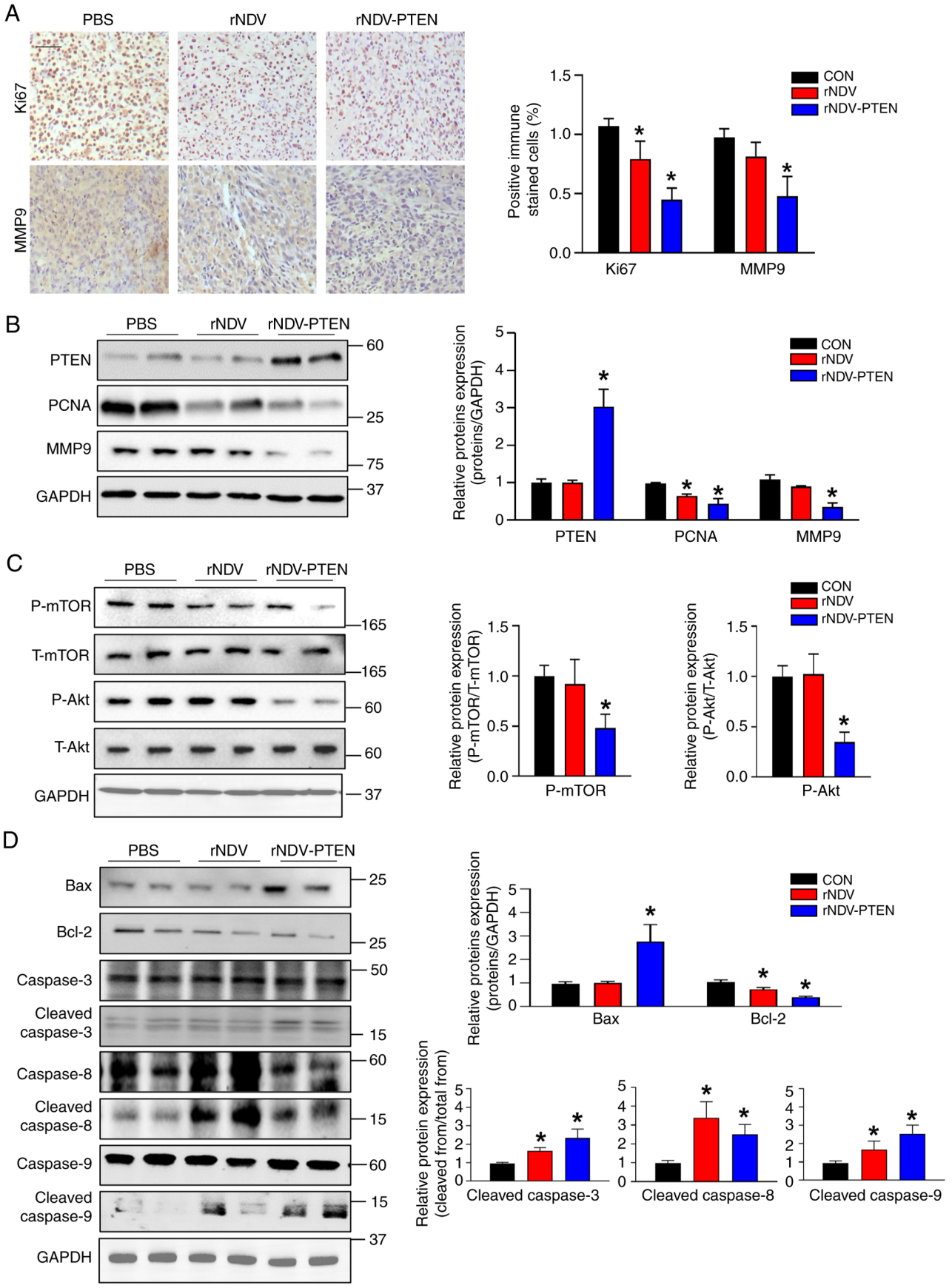

Figure 5. PTEN restoration induces apoptotic cell death by impacting mTOR signaling and autophagy in the orthotopic GBM mouse model. (A) Immunohistochemical staining of Ki-67 (tumor cell proliferation marker) and MMP9 in the GBM orthotopic mouse tissue. Scale bar, 50 μm. (B) PCNA and MMP9 levels, (C) proteins related to the mTOR signaling pathway and autophagy, and (D) apoptosis markers were assessed using immunoblotting in GBM tissue. These data are expressed as the fold change in expression compared with PBS injected mice. GAPDH was used as an internal control. *P<0.05 vs. PBS-injected mice. PTEN, phosphatase and tensin homolog; MMP9, matrix metallopeptidase 9; PCNA, proliferating cell nuclear antigen; GBM, glioblastoma; CON, control.

safety of rNDV-PTEN in patients with GBM. Secondly, while rNDV-PTEN demonstrated its ability to cross the blood-brain barrier in animal models, the precise mechanisms facilitating this process remain unclear and warrant further investigation. Lastly, the heterogeneity of GBM tumors presents a challenge, as PTEN deficiency is not uniform across all GBM cases. Therefore, the therapeutic benefits of rNDV-PTEN may vary depending on the molecular profile of the tumor, which highlights the need for personalized treatment strategies based on genetic screening. NDV induces cancer cell death through multiple mechanisms, including apoptosis, autophagy and necroptosis, and has been reported to enhance the antitumor immune response (43). A critical challenge in GBM treatment is the BBB, a highly selective barrier that restricts the entry of therapeutic agents into the brain. The BBB is composed of BMECs, astrocytes and pericytes, forming tight junctions that prevent non-selective entry of substances (19). The present study aimed to determine whether rNDV-PTEN could cross the BBB and deliver PTEN to GBM cells effectively.

The present study selected U87-MG cells as it has been reported that 30-40% of GBM patients with PTEN gene mutations exhibit low PTEN protein expression, which is associated with a poorer prognosis compared with that in patients without PTEN mutations (44,45). Furthermore, mutation or depletion of PTEN leads to an increase in GBM progression. Low expression level of PTEN mediates poor prognosis in GBM and by increasing proliferation and invasion, it eventually promotes the malignancy of tumor cells (11,46). Moreover, the loss of PTEN function is associated with more aggressive tumors and resistance to conventional therapies (47). Given the results of the present study with this significant subset of GBM cases, the findings suggest that rNDV-PTEN could serve as a promising therapeutic strategy for patients with PTEN-deficient tumors. The ability of rNDV-PTEN to restore PTEN expression in U87-MG cells and inhibit the AKT/mTOR signaling pathway, leading to the inhibition of cell migration and apoptosis, emphasizes its potential efficacy in the GBM cells. Therefore, the present study highlights the relevance and potential impact of rNDV-PTEN as a targeted therapy for PTEN-deficient tumors.

Furthermore, the results of the present study demonstrated that rNDV-PTEN treatment significantly restored PTEN expression in U87-MG cells or the orthotopic mouse model, leading to decreased cell proliferation and migration, and induced apoptosis through the inhibition of the AKT/mTOR signaling pathway (Figs. 2B and 5B). rNDV is an intrinsic oncolytic virus that has been reported to have tumor-selective replication capabilities, resulting in lysis and apoptosis in several cancer cell types (43,48). Indeed, the results of the present study also confirmed that treatment with rNDV alone increased apoptosis compared with no treatment in U87-MG cells or PBS-treated mice. However, despite the apoptosis-inducing effects of rNDV, the present study aimed to further enhance its antitumor efficacy by modifying rNDV to deliver the tumor suppressor gene PTEN, thereby restoring PTEN protein levels. This modification not only amplified the apoptosis signaling pathways but also led to a significant reduction in the expression of cancer metastasis factors. Specifically, in cells treated with rNDV-PTEN, the present study observed a more pronounced increase in pro-apoptotic markers such as Bax and cleaved caspases 3, 8 and 9 (Figs. 2C and 5D) compared with treatment with rNDV alone. These findings are consistent with previous studies that have reported PTEN restoration can inhibit tumor growth and enhance apoptosis in several cancer models (49,50).

In vivo imaging and histological analysis of the orthotopic GBM mouse model demonstrated that rNDV-PTEN treatment resulted in a significant reduction in tumor size compared with controls. MRI and IVIS imaging confirmed that rNDV-PTEN could effectively target and reduce GBM growth in the brain (Figs. 3E and 4A). Notably, the present study did not detect any disruption of the BBB tight junctions following rNDV-PTEN treatment, as demonstrated by MRI and protein expression analyses. This indicates that rNDV-PTEN can cross the BBB without compromising its integrity, likely through a transcellular pathway similar to that used by SARS-CoV-2 (18). The ability of rNDV-PTEN to cross the BBB and deliver PTEN directly to GBM cells is a significant finding (Figs. 4A and S3). Traditional gene therapy vectors, such as adenoviruses or adeno-associated viruses, cannot effectively cross the BBB and are limited by potential immunogenicity and host genome integration issues (51). In contrast, NDV offers a safer and potentially more effective delivery mechanism, particularly for brain tumors.

PTEN serves a crucial role in regulating cell proliferation and migration, and its loss or mutation is associated with a poor prognosis in patients with GBM (52). By restoring PTEN expression, rNDV-PTEN treatment inhibits the AKT/mTOR signaling pathway, reducing tumor growth and enhancing the effectiveness of conventional therapies (53). The mechanism by which rNDV-PTEN induces apoptosis in GBM cells involves the inhibition of the AKT/mTOR pathway. The AKT/mTOR pathway is a critical regulator of cell survival, proliferation and metabolism, and its dysregulation is common in many cancers, including GBM (54). PTEN negatively regulates this pathway by dephosphorylating phosphatidylinositol-3,4,5-trisphosphate, thereby preventing AKT activation. In the present study, rNDV-PTEN treatment restored PTEN expression, leading to decreased phosphorylation of AKT and mTOR, increased levels of pro-apoptotic markers, and reduced cell proliferation and migration.

Additionally, the findings of the present study suggest that rNDV-PTEN treatment can modulate the tumor microenvironment by reducing angiogenesis and metastasis. Histological analysis revealed decreased expression of angiogenic markers and metastasis markers in rNDV-PTEN-treated tumors (Fig. 5A and B). Moreover, the data indirectly indicated that rNDV-PTEN could cross the BBB, as demonstrated by the expression of the NDV-HN and PTEN protein (transgene) in brain tumor tissues detected through immunohistochemistry analysis (Fig. 4A and B). No changes in the tight junction proteins and mRNA (Fig. S2A and B) suggests that the virus could infect a transcellular, rather than paracellular, mechanism to cross the BBB, a hypothesis supported by similar findings in SARS-CoV-2 research (18). However, the present study did not directly observe the movement of viruses using fluorescent markers such as luciferase, indicating that the conclusions of the present study are based on indirect evidence. Despite these promising results, further research is needed to fully understand the mechanism by which NDV crosses the BBB and optimize the delivery system for clinical applications. Future studies should focus on elucidating the pathways involved in NDV transcytosis across the BBB and exploring the potential

of combining rNDV-PTEN with other therapeutic modalities to enhance its efficacy. Additionally, long-term studies are needed to evaluate the safety and efficacy of rNDV-PTEN in clinical settings and to determine the potential for resistance development to this therapeutic approach.

In conclusion, the findings of the present study demonstrate that rNDV-PTEN is a potent oncolytic virus capable of crossing the BBB and delivering the PTEN gene to GBM cells, thereby inducing apoptosis and inhibiting tumor growth. Inhibition of the AKT/mTOR pathway and subsequent activation of pro-apoptotic markers indicates the potential of rNDV-PTEN as a novel therapeutic agent for treating GBM, particularly in patients with PTEN mutations or low PTEN expression. These results provide a strong foundation for further development and clinical testing of rNDV-PTEN as a promising treatment for GBM.

Acknowledgements

Not applicable.

Funding

The present research was supported by the research fund of Chungnam National University and by the Technology Development Program, funded by the Ministry of SMEs and Startups (grant no. S3271268).

Availability of data and materials

The data generated in the present study may be requested from the corresponding author.

Authors' contributions

HJ initiated and designed the study. SK and BKJ performed most of the experiments. SK, BKJ and HJ wrote the manuscript. JK and MK performed certain parts of the experiments. SHJ, JHJ and CSK were responsible for managing and processing data and performing quality checks to ensure data accuracy and consistency. HJ supervised the study. All authors have read and approved the final manuscript. HJ and SK confirm the authenticity of all the raw data.

Ethics approval and consent to participate

All animal studies were approved by and performed and in the animal facility following the guidelines of the Institutional Animal Use and Care Committee of Chungnam National University Hospital (Daejeon, Republic of Korea; approval no. CNUH-021-A0042). The animal experiments (*in vivo* experiment) complied with the Animal Research: Reporting of *In Vivo* Experiments guidelines (55).

Patient consent for publication

Not applicable.

Competing interests

The authors declare that they have no competing interests.

References

1. Ostrom QT, Gittleman H, Fulop J, Liu M, Blanda R, Kromer C, Wolinsky Y, Kruchko C and Barnholtz-Sloan JS: CBTRUS statistical report: primary brain and central nervous system tumors diagnosed in the United States in 2008-2012. Neuro Oncol 17 (Suppl 4): iv1-iv62, 2015.
2. Nelson CP, Bloom DA, Kinast R, Wei JT and Park JM: Long-term patient reported outcome and satisfaction after oral mucosa graft urethroplasty for hypospadias. J Urol 174: 1075-1078, 2005.
3. Luchsinger JA: Type 2 diabetes, related conditions, in relation and dementia: An opportunity for prevention? J Alzheimers Dis 20: 723-736, 2010.
4. Koide S, Koide A and Lipovšek D: Target-binding proteins based on the 10th human fibronectin type III domain (^{10}Fn3). Methods Enzymol 503: 135-156, 2012.
5. Maehama T and Dixon JE: The tumor suppressor, PTEN/MMAC1, dephosphorylates the lipid second messenger, phosphatidylinositol 3,4,5-trisphosphate. J Biol Chem 273: 13375-13378, 1998.
6. Chen JK, Taipale J, Cooper MK and Beachy PA: Inhibition of Hedgehog signaling by direct binding of cyclopamine to Smoothened. Genes Dev 16: 2743-2748, 2002.
7. Choi SW, Lee Y, Shin K, Koo H, Kim D, Sa JK, Cho HJ, Shin HM, Lee SJ, Kim H, *et al*: Mutation-specific non-canonical pathway of PTEN as a distinct therapeutic target for glioblastoma. Cell Death Dis 12: 374, 2021.
8. Golovina VA and Blaustein MP: Spatially and functionally distinct Ca2+ stores in sarcoplasmic and endoplasmic reticulum. Science 275: 1643-1648, 1997.
9. van Noort J, Verbrugge S, Goosen N, Dekker C and Dame RT: Dual architectural roles of HU: Formation of flexible hinges and rigid filaments. Proc Natl Acad Sci USA 101: 6969-6974, 2004.
10. Chen C, Zhu S, Zhang X, Zhou T, Gu J, Xu Y, Wan Q, Qi X, Chai Y, Liu X, *et al*: Targeting the synthetic vulnerability of PTEN-deficient glioblastoma cells with MCL1 inhibitors. Mol Cancer Ther 19: 2001-2011, 2020.
11. Du L, Zhang Q, Li Y, Li T, Deng Q, Jia Y, Lei K, Kan D, Xie F and Huang S: Research progress on the role of PTEN deletion or mutation in the immune microenvironment of glioblastoma. Front Oncol 14: 1409519, 2024.
12. Chen H, Mei L, Zhou L, Shen X, Guo C, Zheng Y, Zhu H, Zhu Y and Huang L: PTEN restoration and PIK3CB knockdown synergistically suppress glioblastoma growth in vitro and in xenografts. J Neurooncol 104: 155-167, 2011.
13. Chen Z, Varney ML, Backora MW, Cowan K, Solheim JC, Talmadge JE and Singh RK: Down-regulation of vascular endothelial cell growth factor-C expression using small interfering RNA vectors in mammary tumors inhibits tumor lymphangiogenesis and spontaneous metastasis and enhances survival. Cancer Res 65: 9004-9011, 2005.
14. Jiang K, Song C, Kong L, Hu L, Lin G, Ye T, Yao G, Wang Y, Chen H, Cheng W, *et al*: Recombinant oncolytic Newcastle disease virus displays antitumor activities in anaplastic thyroid cancer cells. BMC Cancer 18: 746, 2018.
15. García-Romero N, Palacín-Aliana I, Esteban-Rubio S, Madurga R, Rius-Rocabert S, Carrión-Navarro J, Presa J, Cuadrado-Castano S, Sánchez-Gómez P, García-Sastre A, *et al*: Newcastle disease virus (NDV) oncolytic activity in human glioma tumors is dependent on CDKN2A-type I IFN gene cluster codeletion. Cells 9: 1405, 2020.
16. Burman B, Pesci G and Zamarin D: Newcastle disease virus at the forefront of cancer immunotherapy. Cancers (Basel) 12: 3552, 2020.
17. Csatary LK, Gosztonyi G, Szeberenyi J, Fabian Z, Liszka V, Bodey B and Csatary CM: MTH-68/H oncolytic viral treatment in human high-grade gliomas. J Neurooncol 67: 83-93, 2004.
18. Zhang L, Zhou L, Bao L, Liu J, Zhu H, Lv Q, Liu R, Chen W, Tong W, Wei Q, *et al*: SARS-CoV-2 crosses the blood-brain barrier accompanied with basement membrane disruption without tight junctions alteration. Signal Transduct Target Ther 6: 337, 2021.
19. Abbott NJ, Rönnbäck L and Hansson E: Astrocyte-endothelial interactions at the blood-brain barrier. Nat Rev Neurosci 7: 41-53, 2006.
20. Jang SH, Jung BK, An YH and Jang H: The phosphatase and tensin homolog gene inserted between NP and P gene of recombinant New castle disease virus oncolytic effect test to glioblastoma cell and xenograft mouse model. Virol J 19: 21, 2022.

21. Oka N, Soeda A, Inagaki A, Onodera M, Maruyama H, Hara A, Kunisada T, Mori H and Iwama T: VEGF promotes tumorigenesis and angiogenesis of human glioblastoma stem cells. Biochem Biophys Res Commun 360: 553-559, 2007.
22. Mao P, Joshi K, Li J, Kim SH, Li P, Santana-Santos L, Luthra S, Chandran UR, Beno PV, Smith L, *et al*: Mesenchymal glioma stem cells are maintained by activated glycolytic metabolism involving aldehyde dehydrogenase 1A3. Proc Natl Acad Sci USA 110: 8644-8649, 2013.
23. Lin W, Niu R, Park SM, Zou Y, Kim SS, Xia X, Xing S, Yang Q, Sun X, Yuan Z, *et al*: IGFBP5 is an ROR1 ligand promoting glioblastoma invasion via ROR1/HER2-CREB signaling axis. Nat Commun 14: 1578, 2023.
24. Spearman C: The method of 'right and wrong cases' (constant stimuli) without gauss's formula. Br J Psychol 2: 227-242, 1908.
25. Kärber G: Beitrag zur kollektiven behandlung pharmakologischer reihenversuche. Naunyn Schmiedebergs Arch Exp Pathol Pharmakol 162: 480-483, 1931.
26. Livak KJ and Schmittgen TD: Analysis of relative gene expression data using real-time quantitative PCR and the 2(-Delta Delta C(T)) method. Methods 25: 402-408, 2001.
27. Raftery N and Stevenson NJ: Advances in anti-viral immune defence: Revealing the importance of the IFN JAK/STAT pathway. Cell Mol Life Sci 74: 2525-2535, 2017.
28. Zhou S, Wang H, Huang Y, Wu Y and Lin Z: The global change of gene expression pattern caused by PTEN mutation affects the prognosis of glioblastoma. Front Oncol 12: 952521, 2022.
29. Li Y, Liang Y, Sun Z, Xu K, Fan X, Li S, Zhang Z, Jiang T, Liu X and Wang Y: Radiogenomic analysis of PTEN mutation in glioblastoma using preoperative multi-parametric magnetic resonance imaging. Neuroradiology 61: 1229-1237, 2019.
30. Hernandez J, Bonnedahl J, Eliasson I, Wallensten A, Comstedt P, Johansson A, Granholm S, Melhus A, Olsen B and Drobni M: Globally disseminated human pathogenic Escherichia coli of O25b-ST131 clone, harbouring blaCTX-M-15, found in Glaucous-winged gull at remote Commander Islands, Russia. Environ Microbiol Rep 2: 329-332, 2010.
31. Strzalka W and Ziemienowicz A: Proliferating cell nuclear antigen (PCNA): A key factor in DNA replication and cell cycle regulation. Ann Bot 107: 1127-1140, 2011.
32. Wilhelm SM, Collier IE, Marmer BL, Eisen AZ, Grant GA and Goldberg GI: SV40-transformed human lung fibroblasts secrete a 92-kDa type IV collagenase which is identical to that secreted by normal human macrophages. J Biol Chem 264: 17213-17221, 1989.
33. Yang JM, Schiapparelli P, Nguyen HN, Igarashi A, Zhang Q, Abbadi S, Amzel LM, Sesaki H, Quiñones-Hinojosa A and Iijima M: Characterization of PTEN mutations in brain cancer reveals that pten mono-ubiquitination promotes protein stability and nuclear localization. Oncogene 36: 3673-3685, 2017.
34. Cheung M and Testa JR: Diverse mechanisms of AKT pathway activation in human malignancy. Curr Cancer Drug Targets 13: 234-244, 2013.
35. Fine HA: Radiotherapy plus adjuvant temozolomide for the treatment of glioblastoma-a paradigm shift. Nat Clin Pract Oncol 2: 334-335, 2005.
36. Colón-Thillet R, Jerome KR and Stone D: Optimization of AAV vectors to target persistent viral reservoirs. Virol J 18: 85, 2021.
37. Ferguson MS, Lemoine NR and Wang Y: Systemic delivery of oncolytic viruses: Hopes and hurdles. Adv Virol 2012: 805629, 2012.
38. Belete TM: The current status of gene therapy for the treatment of cancer. Biologics 15: 67-77, 2021.
39. Freeman AI, Zakay-Rones Z, Gomori JM, Linetsky E, Rasooly L, Greenbaum E, Rozenman-Yair S, Panet A, Libson E, Irving CS, *et al*: Phase I/II trial of intravenous NDV-HUJ oncolytic virus in recurrent glioblastoma multiforme. Mol Ther 13: 221-228, 2006.
40. Lemos de Matos A, Franco LS and McFadden G: Oncolytic viruses and the immune system: The dynamic duo. Mol Ther Methods Clin Dev 17: 349-358, 2020.
41. Li X, Sun X, Wang B, Li Y and Tong J: Oncolytic virus-based hepatocellular carcinoma treatment: Current status, intravenous delivery strategies, and emerging combination therapeutic solutions. Asian J Pharm Sci 18: 100771, 2023.
42. Lin D, Shen Y and Liang T: Oncolytic virotherapy: Basic principles, recent advances and future directions. Signal Transduct Target Ther 8: 156, 2023.
43. Zamarin D and Palese P: Oncolytic Newcastle disease virus for cancer therapy: Old challenges and new directions. Future Microbiol 7: 347-367, 2012.
44. Hashemi M, Etemad S, Rezaei S, Ziaolhagh S, Rajabi R, Rahmanian P, Abdi S, Koohpar ZK, Rafiei R, Raei B, *et al*: Progress in targeting PTEN/PI3K/Akt axis in glioblastoma therapy: Revisiting molecular interactions. Biomed Pharmacother 158: 114204, 2023.
45. Zhang P, Meng X, Liu L, Li S, Li Y, Ali S, Li S, Xiong J, Liu X, Li S, *et al*: Identification of the prognostic signatures of glioma with different PTEN status. Front Oncol 11: 633357, 2021.
46. Fraser MM, Zhu X, Kwon CH, Uhlmann EJ, Gutmann DH and Baker SJ: Pten loss causes hypertrophy and increased proliferation of astrocytes in vivo. Cancer Res 64: 7773-7779, 2004.
47. Han F, Hu R, Yang H, Liu J, Sui J, Xiang X, Wang F, Chu L and Song S: PTEN gene mutations correlate to poor prognosis in glioma patients: A meta-analysis. Onco Targets Ther 9: 3485-3492, 2016.
48. Reichard KW, Lorence RM, Cascino CJ, Peeples ME, Walter RJ, Fernando MB, Reyes HM and Greager JA: Newcastle disease virus selectively kills human tumor cells. J Surg Res 52: 448-453, 1992.
49. Islam MA, Xu Y, Tao W, Ubellacker JM, Lim M, Aum D, Lee GY, Zhou K, Zope H, Yu M, *et al*: Author correction: Restoration of tumour-growth suppression in vivo via systemic nanoparticle-mediated delivery of PTEN mRNA. Nat Biomed Eng 2: 968, 2018.
50. Li Y, Zhang P, Qiu F, Chen L, Miao C, Li J, Xiao W and Ma E: Inactivation of PI3K/Akt signaling mediates proliferation inhibition and G2/M phase arrest induced by andrographolide in human glioblastoma cells. Life Sci 90: 962-967, 2012.
51. Pardridge WM: Drug transport across the blood-brain barrier. J Cereb Blood Flow Metab 32: 1959-1972, 2012.
52. Vivanco I and Sawyers CL: The phosphatidylinositol 3-kinase AKT pathway in human cancer. Nat Rev Cancer 2: 489-501, 2002.
53. Huang X, You L, Nepovimova E, Psotka M, Malinak D, Valko M, Sivak L, Korabecny J, Heger Z, Adam V, *et al*: Inhibitors of phosphoinositide 3-kinase (PI3K) and phosphoinositide 3-kinase-related protein kinase family (PIKK). J Enzyme Inhib Med Chem 38: 2237209, 2023.
54. Fruman DA, Chiu H, Hopkins BD, Bagrodia S, Cantley LC and Abraham RT: The PI3K pathway in human disease. Cell 170: 605-635, 2017.
55. Kilkenny C, Browne WJ, Cuthi I, Emerson M and Altman DG: Improving bioscience research reporting: The ARRIVE guidelines for reporting animal research. Vet Clin Pathol 41: 27-31, 2012.

Copyright © 2024 Kim et al. This work is licensed under a Creative Commons Attribution-NonCommercial-NoDerivatives 4.0 International (CC BY-NC-ND 4.0) License.